**P1.20** Simulations of extreme convective storms in future climates: proof-of-concept tests with a retrospective event

Brooke A. Halvorson*, Robert J. Trapp, and Noah S. Diffenbaugh
Purdue University, West Lafayette, Indiana

## 1. INTRODUCTION

Questions regarding changes in frequency, location, and intensity of extreme convective storm events in future climates remain unresolved owing to the inability of typical global (GCM) and regional climate models (RCM) to simulate such events. One could circumvent this problem by using certain storm environmental parameters (e.g. CAPE and shear), based on output from these larger-scale models, as proxies for storm occurrence (e.g. Brooks et al. 2003). Alternatively, one could attempt a direct modeling approach, culminating in cloud-resolving simulations, as is proposed herein.

In this paper, historical (or "retrospective") simulations are used to test whether this telescoping model strategy can, for an extreme convective event, accurately represent the antecedent conditions on the synoptic and mesoscale, the initiation of deep convection, and then the type or mode of the convective storms. We evaluate two approaches applied to the 3-4 April 1974 Tornado Super Outbreak (see also Locatelli et al. 2002): a Weather Forecasting Approach (WFA), in which a global dataset drives a mesoscale and nested cloud-resolving model without the intermediate step of a RCM, and a Regional Climate Modeling Approach (RCMA), in which a global dataset is used to drive long-term regional climate model simulations that in turn drive mesoscale and nested cloud-resolving model simulations. The primary advantage of the WFA is the reduction in model domain boundaries and their deleterious effects. As discussed by Giorgi and Mearns (1999), the RCMA has the advantage of ample time for all important physics components (i.e. radiative transfer, resolvable scale and convective cloud and precipitation processes, boundary layer, and surface physics processes) to interact and equilibrate with the ambient atmosphere.

These simulations will help us begin to assess which approach will lead to the most accurate depiction of the convective mode. This is important since knowledge of mode also provides knowledge of the other hazardous weather (e.g. tornadoes, hail, damaging winds) most likely to accompany the storms.

## 2. EXPERIMENTAL DESIGN

The WFA employs the Weather Research and Forecasting (WRF) Model Version 2.0.3.1 as a mesoscale and cloud-resolving model and is applied to a domain extending east from central Nevada to western Pennsylvania and from northern Wisconsin south to central Mississippi (Fig. 1) with a horizontal gridpoint spacing of 27km. Two-way interactive subdomains of 9km and 3km gridpoint spacing, respectively, are nested within this parent domain. The 3km domain centers on Indiana and western Ohio south to northern Tennessee to capture some of the most intense convective storms of that day, including those that produced a record 148 tornadoes. The model includes 31 vertical levels, and utilizes the Kain-Fritsch cumulus parameterization scheme on the parent domain only. WRF is initialized with T62 resolution (approximately 210km) NCAR/NCEP Global Reanalysis (NNRP) data at 0000 UTC 3 April 1974 (see Kalnay et al., 1996). The NNRP data also provide the WRF model boundary conditions at 6-hour intervals.

The RCMA method utilizes the NNRP data to force the Abdus Salam Institute for Theoretical Physics Regional Climate Model, Version 3, (RegCM3) (see Pal et al. 2005) a hydrostatic,

* *Corresponding author address:* Brooke A. Halvorson, Purdue University, Department of Earth & Atmospheric Sciences, West Lafayette, Indiana 47906; email: halvorso@purdue.edu.

sigma coordinate, primitive equation RCM originally derived from the NCAR/Pennsylvania State University Mesoscale Model Version 4. RegCM3 was run continuously from 1961 to 2000 over a domain encompassing the contiguous United States at a horizontal gridpoint spacing of 55km (Fig. 2). The RegCM3 data provide initial and boundary conditions for the WRF model, which is initialized from these data at 0000 UTC 3 April 1974. The WRF model domains are also configured as in Fig. 1.

## 3. CASE DESCRIPTION

The Tornado Super Outbreak of 3-4 April 1974 is considered to be one of the most devastating tornado outbreak of the 20th century (Hoxit and Chappell 1975; Brooks and Doswell 2001). 148 tornadoes occurred in the Ohio and Tennessee River Valleys between noon CST April 3rd and noon CST April 4th, killing 315 people and injuring over 6,000 others (Hoxit and Chappell 1975).

A strong upper level baroclinic wave moved inland over California and Oregon on the afternoon of 1 April 1974. The wave and associated front propagated east and a squall line developed in central Oklahoma by 0000 UTC on 3 April (3/0000; hereafter, day/hour convention is followed). By 3/1200 the surface low was located in central Kansas with a significant temperature gradient across a total of five frontal boundaries (Fig. 3). According to Hoxit and Chappell (1975), at this time, principal areas of convection were found in the western Carolinas and northern Georgia and central Illinois to western Kentucky and into northeastern Arkansas, in the form of an extensive convective line (Fig. 4). Three squall lines were visible on satellite at 3/1800, and by 3/2100 all three convective lines were producing tornadoes, including the tornado of Xenia, Ohio, reported at 3/2040. At 4/0000 a fourth convective line located over northwestern Indiana was producing almost continuous tornado tracks which included the tornado that devastated Monticello, Indiana. The storms subsequently moved into the southeastern states and twenty additional tornadoes were reported between Virginia and Florida into the afternoon of 4 April.

## 4. RESULTS

We begin with a comparison of the synoptic-scale features simulated using the RCMA and WRF. At 3/0000, the location of the surface low pressure (southeast Colorado/southwest Kansas) and magnitude (983mb) are represented well in the WFA simulation. The RCMA simulated pressure field has the low ~675 km northeast of the observed location (not shown). At subsequent times, the WFA continues to compare favorably to the observations, while the synoptic-scale low in the RCMA remains displaced from the observed location. Frontal positions, as determined by surface temperature, dewpoint, and wind fields, are consistent with the placement of the respective surface low. We note here that some of the discrepancies in the RCMA simulation are probably related to the unavailability of some of the land-surface variables (such as top layer soil moisture) during the WRF initialization; experimentation with such variables is now underway.

The WFA simulates a broad precipitation shield extending from eastern Colorado northeast to central Wisconsin then south through central Illinois; the significant region of precipitation observed in the Carolinas is absent (Fig. 5). The RCMA depicts less precipitation in comparable regions (Fig. 6). Radar summary charts similarly show this broad precipitation area (Fig. 4). Subsequently, the RCMA broad-scale precipitation fields become more consistent with the radar summary charts, in terms of the representation of convective lines (see Figs. 7, 8, and 9). The details in modeled simulated precipitation include cells and convective line segments, with the WFA exhibiting structures that appear more consistent with observations shown by Agee et al. (1975) (Figs. 10 and 11). Note that intense convective storms ultimately form in Illinois, Indiana, and Ohio in both simulations (Figs. 12 and 13), several hours after the time the actual storms were observed.

To begin to assess whether or not the modeled convective cells had supercell characteristics, as observed on this day (see Agee et al. 1975), fields of vertical velocity and vertical vorticity are examined. A rotating updraft, a supercell hallmark, is implied by a high spatial correlation between vertical velocity and vertical vorticity. Indeed, Figs. 14 and 15 show a number of cells in which vertical velocity and vertical vorticity appear to be highly correlated. Such areas in the convective lines imply the potential of the lines to spawn tornadoes. A quantitative measure of the correlation is forthcoming.

## 5. CONCLUSIONS AND FUTURE WORK

A first attempt was made to explicitly simulate the Tornado Super Outbreak of April 3-4, 1974 using two telescoping modeling approaches. Both approaches resulted in intense convective storms – some with apparent supercellular characteristics – in Illinois, Indiana, and Ohio, but several hours past the time actual storms were observed. A detailed analysis of these model solutions, as well as tests with other model configurations, will be pursued.

This work is a proof of concept for a larger initiative that concentrates on changes in convective weather systems, and associated hazardous weather, in past and future climates.

## 6. REFERENCES


Agee, E., C. Church, C. Morris, and J. Snow, 1975: Some Synoptic Aspects and Dynamic Features of Vortices Associated with the Tornado Outbreak of 3 April 1974. *Mon. Wea. Rev.*, **103**, 318-333.

Brooks, H.E., J.W. Lee, and J.P. Craven, 2003: The Spatial Distribution of Severe Thunderstorm and Tornado Environments from Global Reanalysis Data. *Atmos. Res.*, **67-68**, 73-94.

----, and C.A. Doswell: 2001: Normalized Damage from Major Tornadoes in the United States: 1890-1999. *Wea. Forecasting*, **16**, 168-176.

Giorgi, F. and L.O. Mearns, 1999: Introduction to Special Section: Regional Climate Modeling Revisited. *J. Geophy. Res.*, **104**, 6335-6352.

Hoxit, L.R. and C.F. Chappell, 1975: Tornado Outbreak of April 3-4, 1974: Synoptic Analysis. *NOAA Tech. Report*, Boulder, CO.

Kalnay, E., M. Kanamitsu, R. Kistler, W. Collins, D. Deaven, L. Gandin, M. Iredell, S. Saha, G. White, J. Woollen, Y. Zhu, M. Chelliah, W. Ebisuzaki, W. Higgins, J. Janowiak, K.C. Mo, C. Ropelewski, J. Wang, A. Leetmaa, R. Reynolds, R. Jenne, and D. Joseph, 1996: The NCEP/NCAR 40-Year Reanalysis Project. *Bull. Amer. Meteor. Soc.,* **77**, 437-471.

Locatelli, J.D., M.T. Stoelinga, and P.V. Hobbs, 2002: A New Look at the Super Outbreak of Tornadoes on 3-4 April 1974. *Mon. Wea. Rev.*, **130**, 1633-1651.

Pal, J.S., F. Giorgi, X. Bi, N. Elguindi, F. Solmon, X. Gao, M. Ashfaq, R. Francisco, J.L. Bell, N.S. Diffenbaugh, J. Karmacharya, L.C. Sloan, A. Steiner, J.M. Winter, A. Zakey, 2005: The ICTP RegCM3 and RegCNET: Regional climate modeling for the developing world, (submitted to *Bull. of the Amer. Met. Soc.*).

Weiss, S., J. Kain, M. Baldwin, D. Bright, G. Carbin, and J. Hart, 2005: NOAA Hazardous Weather Testbed SPC/NSSL Spring Program 2005 Program Overview and Operations Plan. SPC/NSSL Science Support Area, April 2005.

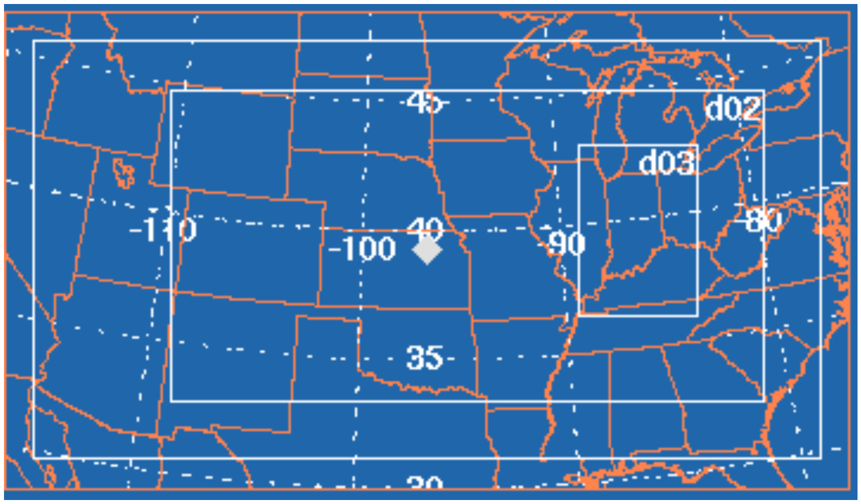


**Figure 1. Domains for WRF model. Domain 1 (d01) has a horizontal gridpoint spacing of 27km, domain 2 (d02) of 9km, and domain 3 (d03) of 3km.**

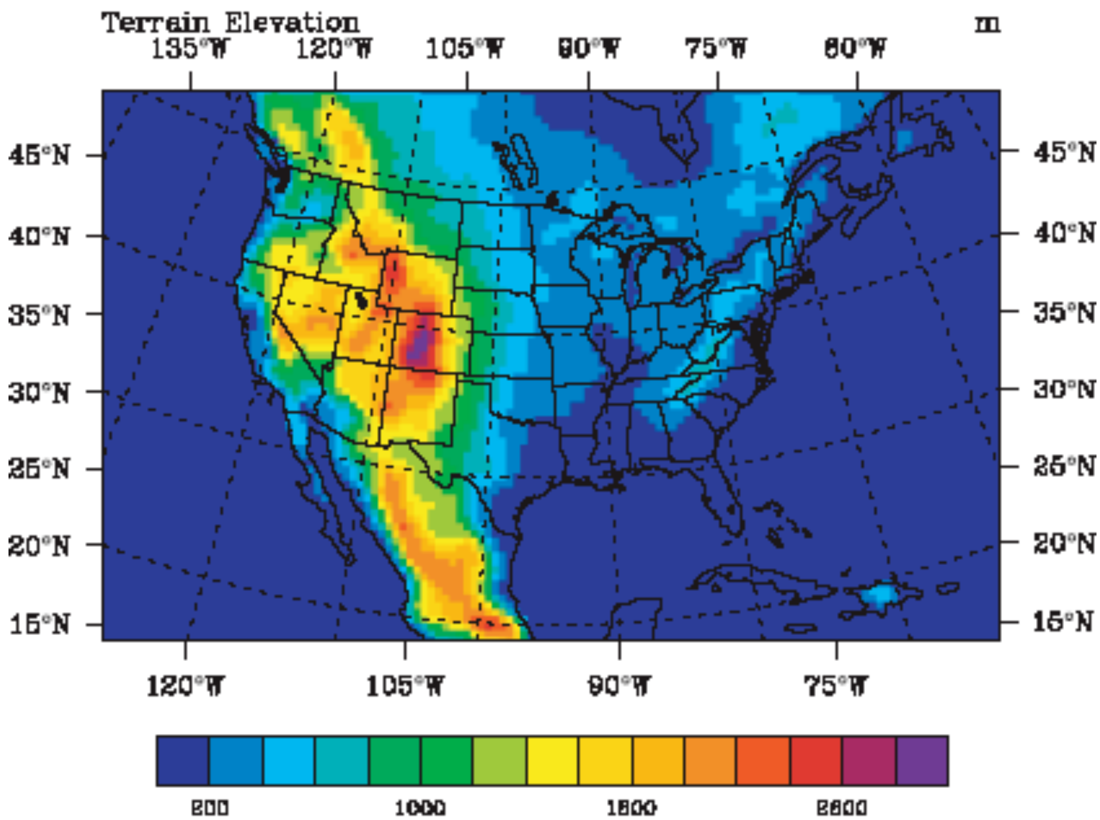


**Figure 2. Domain for RegCM3 has a horizontal gridpoint spacing of 55km and associated terrain elevation in meters.**

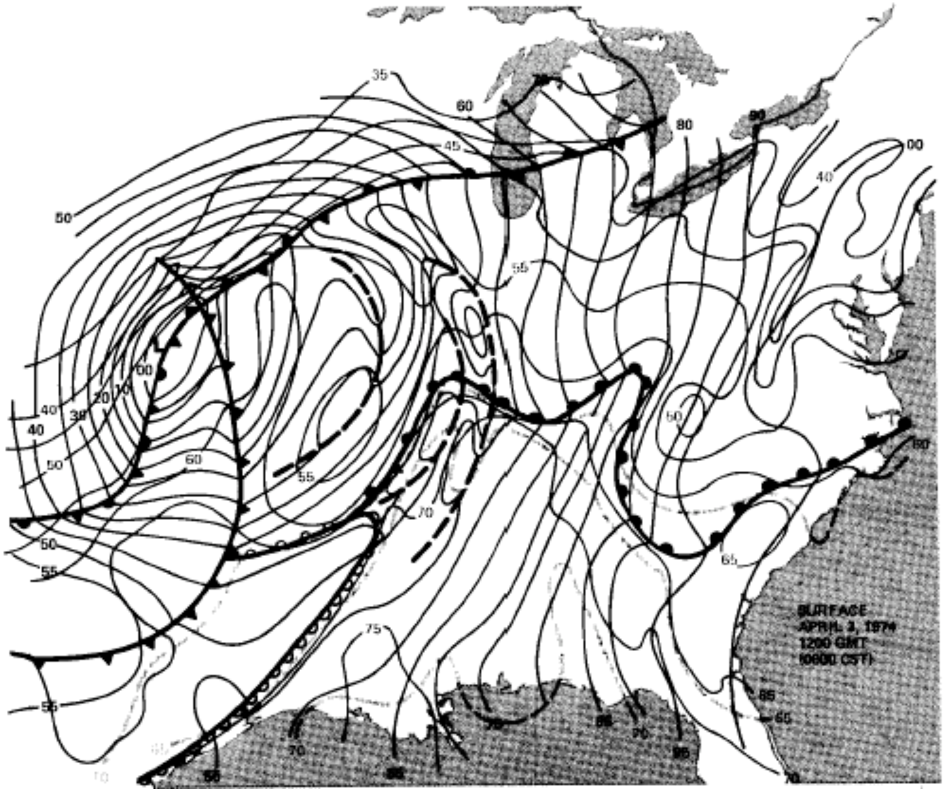


**Figure 3. Surface analysis, valid 1200 UTC 3 April 1974.**
**Altimeter settings in excess of 29.00 inches, 0.05-inches-of-mercury intervals; Isotherms, 5F intervals; Isodrosotherms, 5F intervals for values > 60F; Squall lines, mesoscale troughs, and outflow boundaries, dashed lines (from Hoxit and Chappell 1975).**

**Figure 4. 1125 UTC 3 April 1974 radar summary chart (from Hoxit and Chappell 1975).**

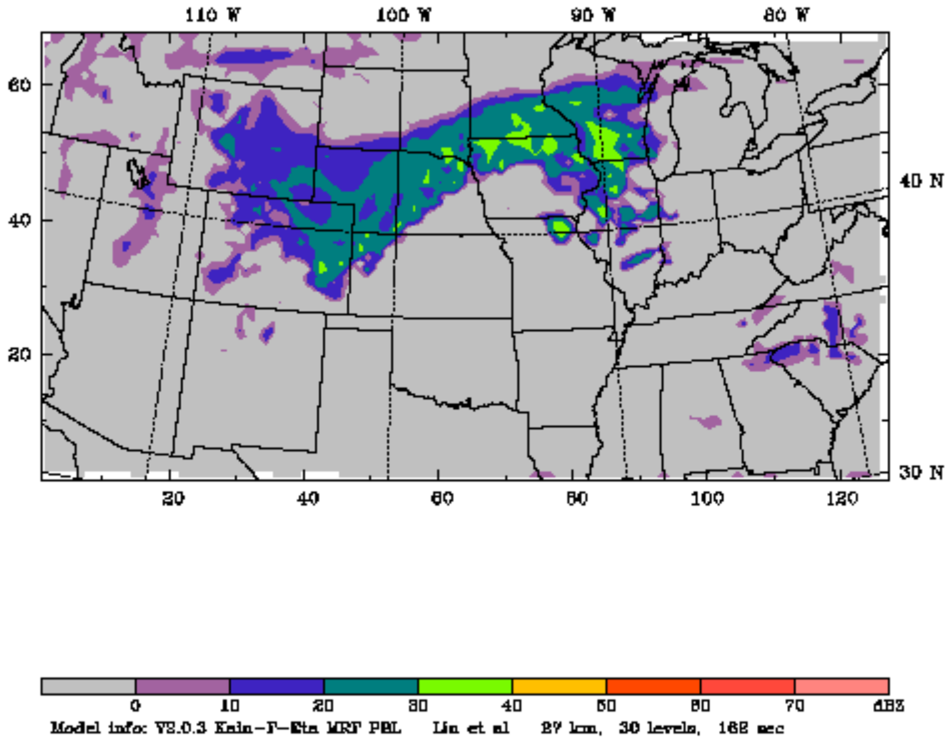


**Figure 5. 1200 UTC 3 April 1974 WFA simulated reflectivity (dBZ), at 1km, on domain 1.**

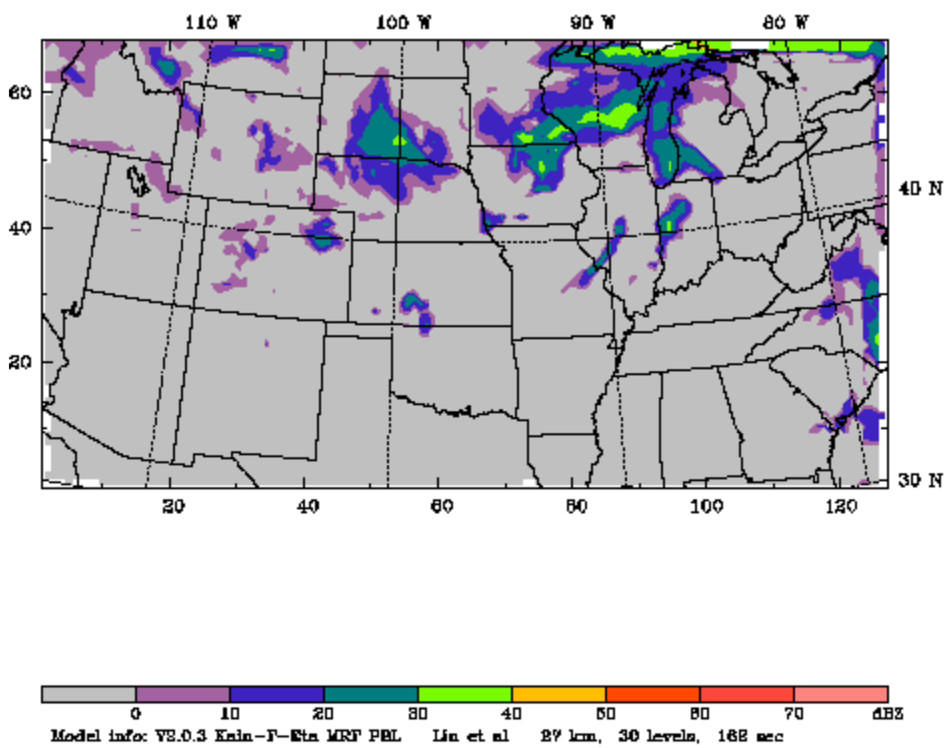


**Figure 6. As in Fig. 5, except for the RCMA simulation.**

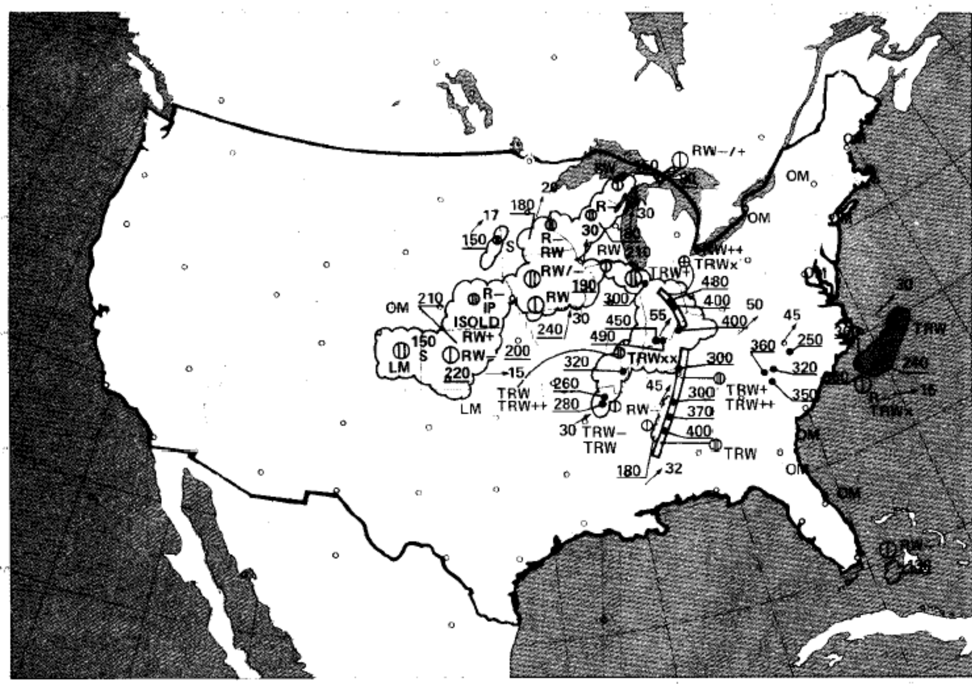

**Figure 7. 1500 UTC 3 April 1974 radar summary chart (from Hoxit and Chappell 1975).**

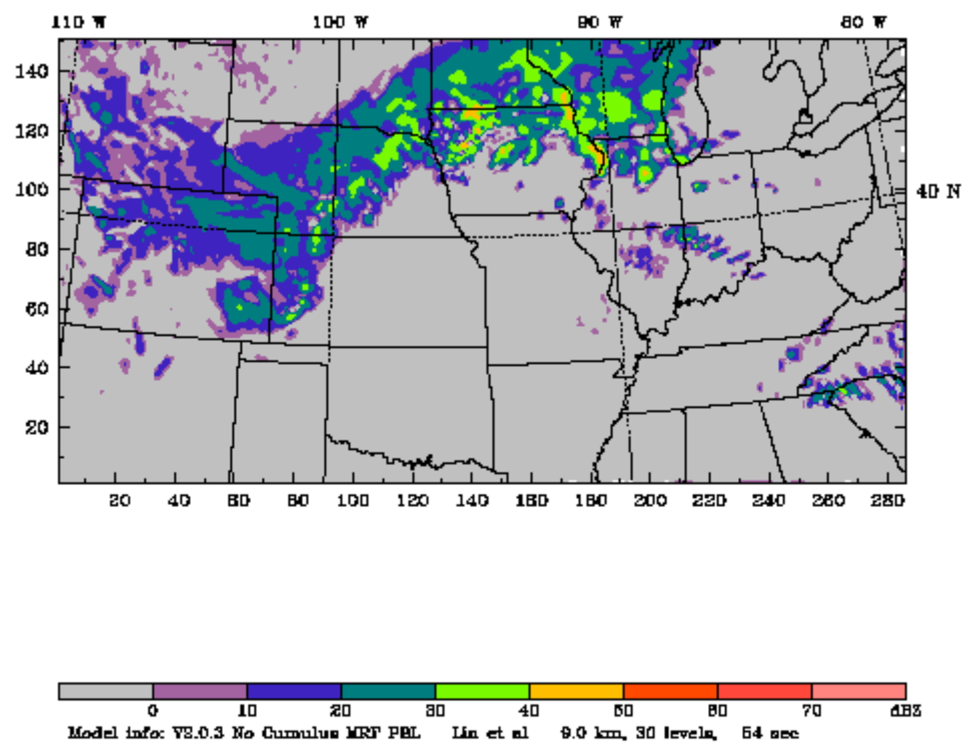


**Figure 8. 1500 UTC 3 April 1974 WFA simulated reflectivity (dBZ) at 1km, on domain 2.**

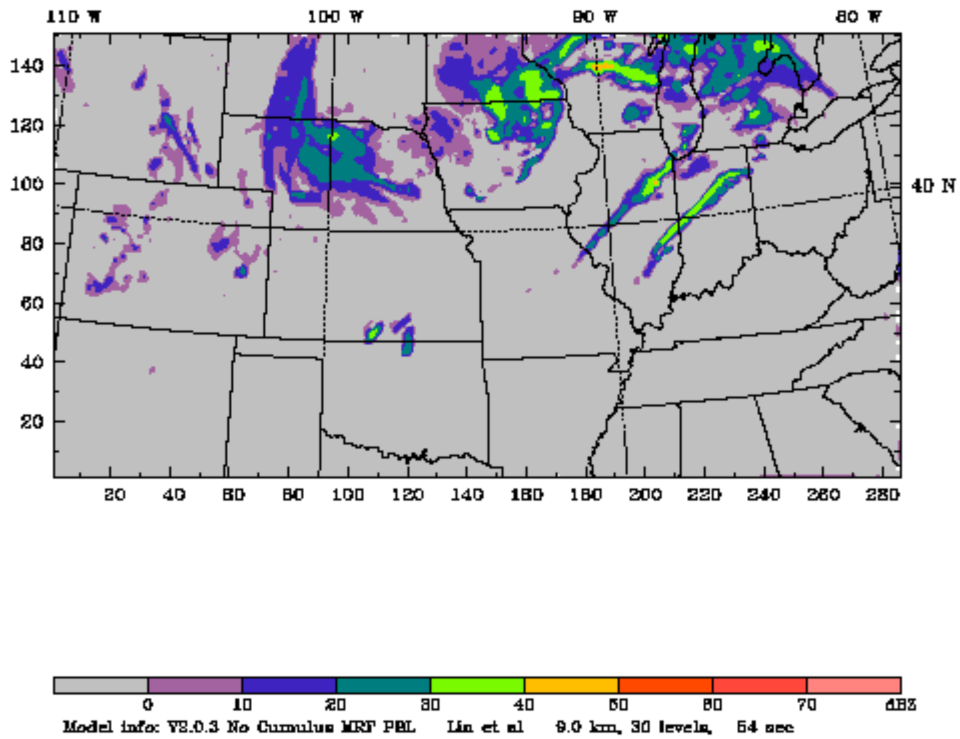


**Figure 9. As in Fig. 8, except for the RCMA simulation.**

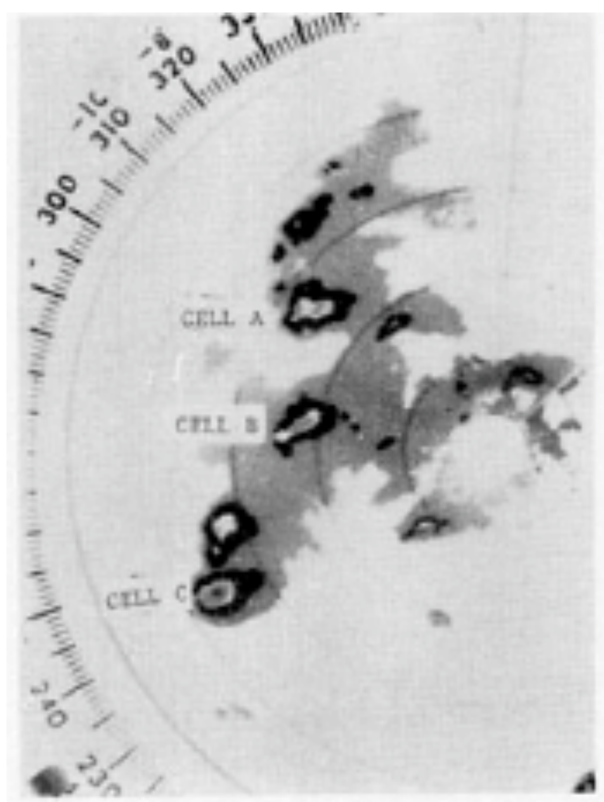


**Figure 10. 1947 UTC 3 April 1974 WSR-57 VIP radar reflectivity display from Covington, KY (125 n mi range) (from Agee et al. 1975)**

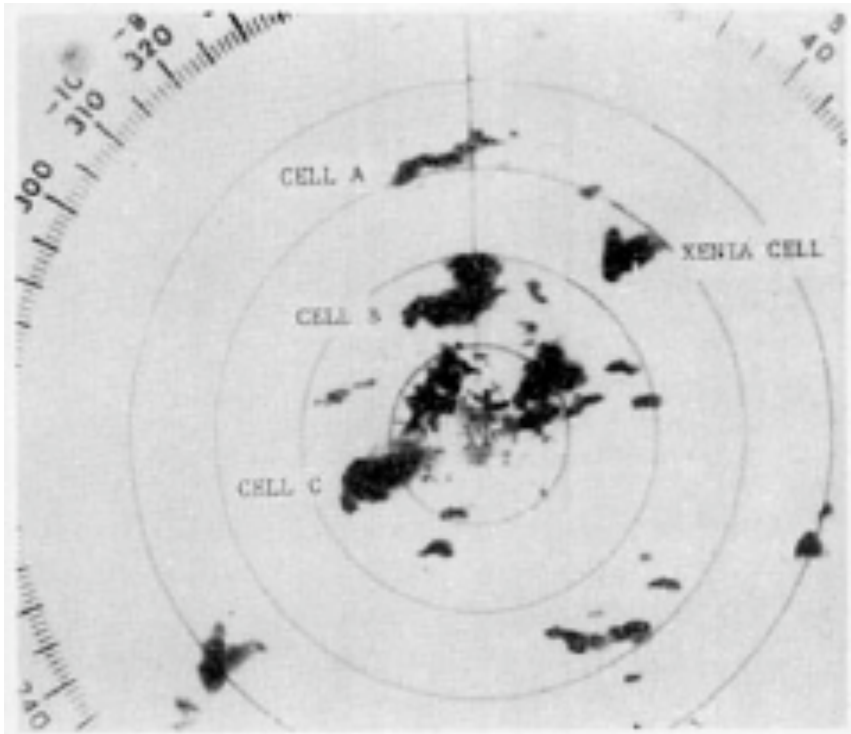


**Figure 11. As in Fig. 10, except at 2001 UTC.**

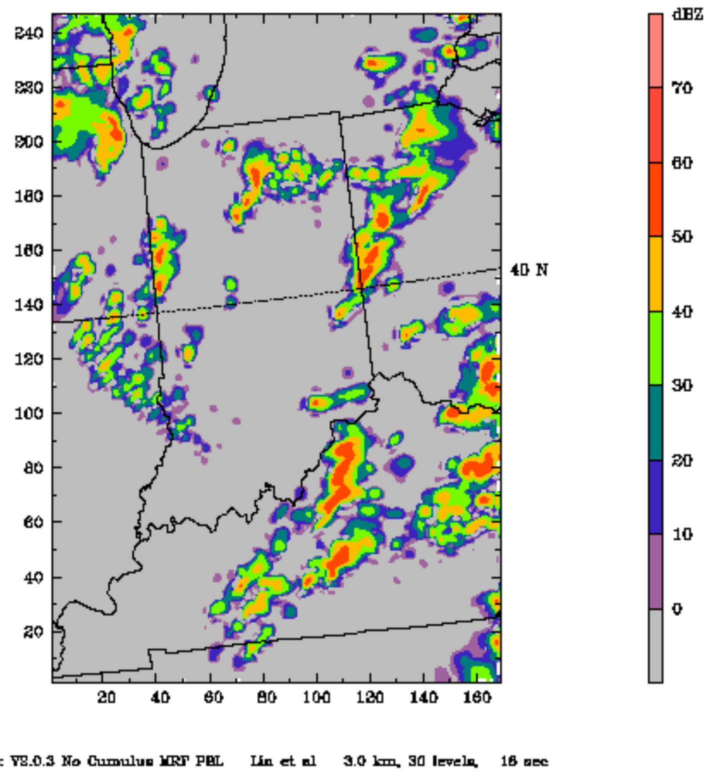


**Figure 12. 0000 UTC 4 April 1974 WFA simulated reflectivity (dBZ) at 1km, for domain 3.**

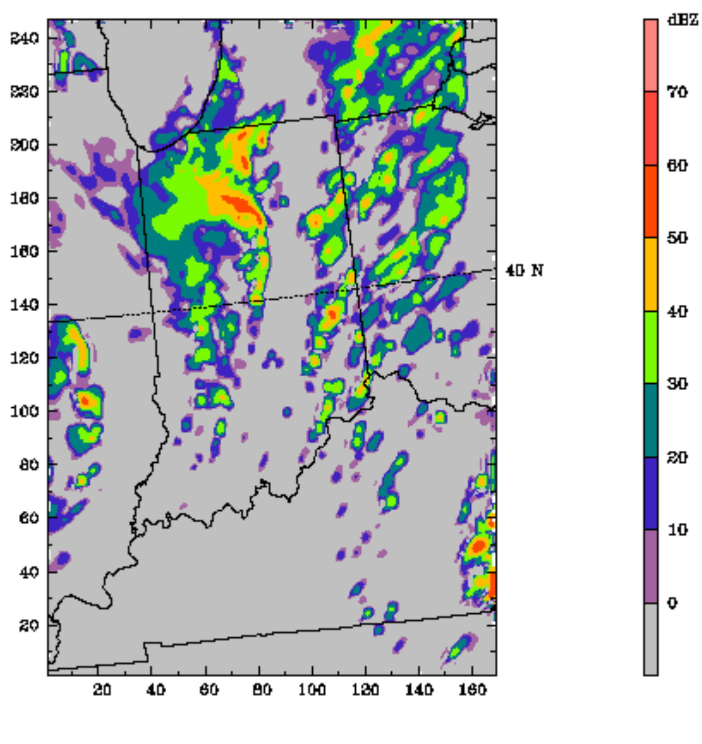


**Figure 13. As in Fig 12, except for the RCMA simulation.**

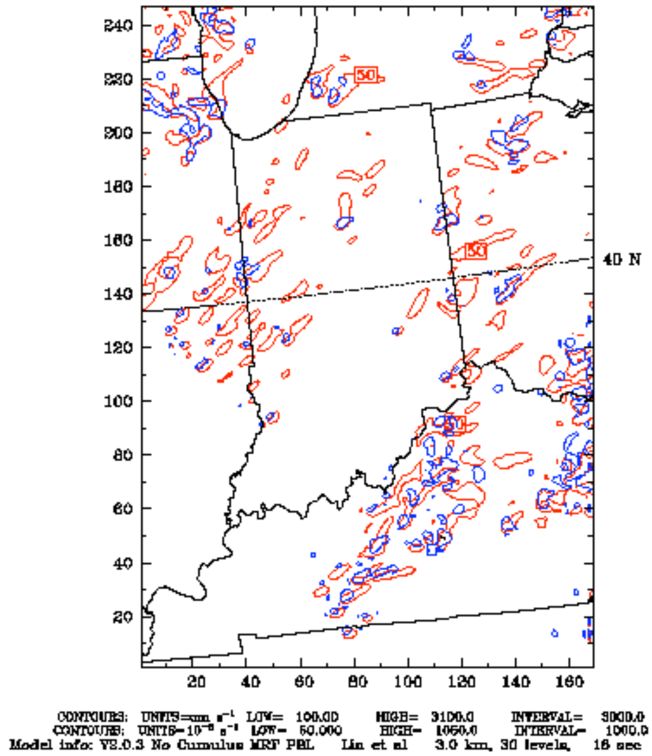


**Figure 14. 0000 UTC 4 April 1974 WFA vertical velocity and vertical vorticity at 5 km, on domain 3. Vertical vorticity (in red) contour at $5x10^{-4}$ $s^{-1}$ interval, vertical velocity (in blue) contour at 1 $ms^{-1}$ interval.**

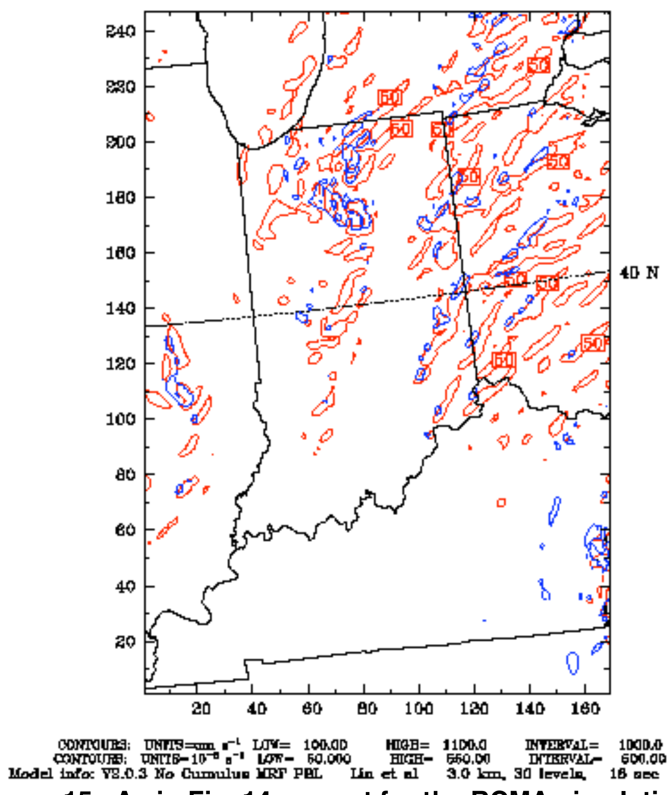


**Figure 15. As in Fig. 14, except for the RCMA simulation.**